A Theoretical Investigation of the Yield-to-Damage Enhancement with Polyatomic Projectiles in Organic SIMS

T. C. Nguyen, David W. Ward, Jennifer A. Townes, Anna K. White, and Kristin D. Krantzman*

Department of Chemistry and Biochemistry, College of Charleston, Charleston, South Carolina, 29424-001

Barbara J. Garrison

Department of Chemistry, 152 Davey Laboratory, The Pennsylvania State University, University Park, Pennsylvania 16802

Received: March 22, 2000; In Final Form: June 21, 2000

Experiments show that polyatomic projectiles have the potential to improve the sensitivity of organic secondary ion mass spectrometry by increasing the yield without a comparable increase in damage to the sample. Molecular dynamics simulations of the high energy bombardment of an organic film have been performed with the purpose of understanding how the yield-to-damage ratio is enhanced with polyatomic projectiles. The model systems consist of 0.6 keV Xe and SF_5 projectiles bombarding a monolayer of biphenyl molecules on two different substrates, Cu(100) and Si(001). The yield-to-damage ratio is the ratio of the yield, defined as the number of molecules ejected stable and intact, to the damage, defined as the sum of molecules ejected either fragmented or unstable. To have a quantity that is comparable to the experimental definition of damage cross section, a yield-to-disappearance ratio, defined as the ratio of the yield to the sum of the yield and damage, is also calculated. The enhancements in both the yield-to-damage and yield-to-disappearance ratios show the same trends, with the greatest enhancement on the substrate with the open lattice structure and the lighter mass atoms, ^{12}Si(100). Polyatomic projectiles are able to increase the yield more than the damage because different types of motion are responsible for the production of the two types of molecules. The yield is enhanced when the polyatomic projectile deposits energy into upward moving substrate atoms over a wider surface area, which leads to a greater number of intact and stable molecules ejected from the surface. Damage to molecules is caused primarily by the impact of the bombarding projectile.

1. Introduction

Secondary ion mass spectrometry (SIMS) can be used to analyze high-molecular-weight nonvolatile organic compounds that cannot be analyzed by traditional methods.[1−5] A keV primary ion beam bombards the sample consisting of the molecules to be analyzed on a solid substrate or in solid form, and the secondary ion emission of molecular ions is measured. Low primary ion doses must be used to minimize damage to the sample, and therefore, the sensitivity depends on increasing the secondary ion emission (SIE) yield per each primary ion impact. There has been considerable interest in the use of polyatomic ions as a primary ion source because they have been shown to increase the yield of desorbed molecular ions by an order of magnitude or more.[6−25]

Recently, there have been numerous experiments with SF_5^+, which has become available as a primary ion source.[26−32] The most dramatic enhancements in yield have been observed by Kötter and Benninghoven, who measured the yield from bulk and spin-coated polymer surfaces with 10 keV Ar^+, Xe^+, and SF_5^+ ions. The yield with SF_5^+ compared to Ar^+ was found to be up to 1000 times greater with the polyatomic projectile.[26] The enhancements on monolayer targets, however, are substantially less than on bulk molecular solids. For example, Stapel et al. measured yields with Ar^+, Xe^+, Ga^+, and SF_5^+ on monolayer and multilayer Langmuir−Blodgett films and found the enhancement to be considerably less on the monolayer films.[27] Ada and Hanley measured ion yields from a surface composed of NH_3 physisorbed to a CO monolayer on Ni and found SF_5^+ to produce only a factor of 2 greater yield than Xe^+.[28] Van Stipdonk et al. have examined the effect of the number of layers on the ion yield with $(CsI)_nCs^+$ ($n = 0-2$) projectiles.[21] They created a monolayer of anions by exchanging tetrafluoroborate and tetraphenylborate anions to the surface of an amine-terminated self-assembled monolayer. The yield with the monolayers was compared to that obtained by bombarding bulk inorganic targets of solid $NaBF_4$ and $NaB(Ph_4)$. Nonlinear enhancements were observed with the bulk targets, while only a slight nonlinear enhancement was observed with the exchanged monolayers.

An issue more critical than the yield enhancement is whether polyatomic projectiles increase the useful signal. For polyatomic ions to be advantageous, the increase in damage by the polyatomic ion must be less than the increase in yield. In their pioneering work, Appelhans and Delmore performed experiments with Cs^+ and $SF_6°$ on a tetrahexylammonium bromide target. The damage cross section is determined by measuring the decay in signal intensity as a function of beam fluence and measures the total number of molecules that are removed from the surface, regardless of whether they are detected as yield. The increase in yield with $SF_6°$ was slightly greater than the increase in damage cross section.[6] A later study compared yields

* To whom correspondence should be addressed. E-mail: krantzmank@cofc.edu.

10.1021/jp001089y CCC: $19.00
Published on Web 08/02/2000

and damage cross sections with Cs^+ and ReO_4^- ions on sodium nitrate and found the yield to be greater and the damage cross section to be less with the polyatomic ion.[7] In the experiments by Kötter and Benninghoven on polymeric surfaces, more fragmentation was observed with the polyatomic projectile, but the damage cross section was found to increase less than the corresponding yield.[26]

Van Stipdonk and co-workers have discovered another interesting aspect of the damage created by polyatomic ions.[15−21] They have found that polyatomic ions produce a greater number of "manufactured" ions that do not reflect the structure of the material to be analyzed and may lead to errors in the interpretation of the mass spectra. For example, experiments were performed with $(CsI)_nCs^+$ ($n = 0-2$) and C_{60}^+ ions on a $NaBF_4$ target.[18] In addition to a series of ions containing BF_4^-, a series of ions containing NaF was also observed. Na^+ is not bonded to F^- in the target surface, and therefore the production of NaF is produced by the rearrangement of target atoms. The increase in yield of ions produced by rearrangement of atoms on the surface is greater than the increase in analytically useful ions and increases as the number of atoms in the projectile increases.

Experimentalists have hypothesized how polyatomic projectiles are able to enhance the secondary ion yield. Benninghoven proposed that the energy density deposited in the surface must be within a definite range in order for molecules to desorb intact and stable.[1,33] Molecules very close to the impact point receive too much energy and are fragmented by the impact. Molecules far out from the impact point are not affected. Only molecules within a certain annular region receive the correct amount of energy to desorb intact and stable from the surface. Appelhans and Delmore hypothesized that polyatomic projectiles increase the emission yield by increasing the energy density deposited near the surface.[6] After the projectile splits into atoms, collision cascades created by the atoms overlap in space, and therefore, a greater surface area is affected by the impact, leading to an enhancement in yield. This hypothesis, however, does not explain why there would be a greater increase in yield than damage with the polyatomic projectile.

Previously, we have performed molecular dynamics simulations in order to examine the effect of polyatomic projectiles on the yield.[34−38] The blending of molecular dynamics simulations with the availability of multi-body potentials has proven successful in the modeling of the high-energy bombardment of organic monolayers on metal surfaces.[39−47] In the first study, a model system consisting of a single biphenyl molecule on a Cu(001) surface was bombarded with energetic Cu_n ($n = 1-4$) clusters.[34,35] A cooperative mechanism was found to be responsible for an enhancement in yield with polyatomic projectiles in which adjacent collision cascades hit different parts of the molecule and collaborate to eject the intact molecule from the surface. Simulations were extended to a more realistic system consisting of a monolayer of biphenyl molecules on a Cu(001) substrate.[36] The yield increased only linearly with cluster size, but the yield-to-damage ratio increased with cluster size, indicating that clusters have the potential to improve the sensitivity of SIMS.

Preliminary simulations with Xe and SF_5 clusters were performed on a monolayer of biphenyl molecules on two different substrates: Cu(001) and Si(100).[37] The effect of the number of atoms in the projectile can be measured by comparing yields with SF_5 and Xe at the same incident energy because the two projectiles have approximately the same mass. The enhancement in yield depends strongly on the structure of the lattice. The breakup of the SF_5 cluster within the more open lattice of the Si(100) substrate initiates collision cascades that lead to substrate atoms hitting the biphenyl molecules from below, which result in a greater yield of ejected molecules. Contour plots of the energy density distribution for a few typical trajectories show that SF_5 produces a larger area of energy density than Xe.[38] The increase in area with SF_5 is more pronounced on the silicon substrates, which accounts for the greater enhancement in yield.

The purpose of the present work is to understand how polyatomic projectiles can increase the yield more than the damage. Simulations of the bombardment of a monolayer of biphenyl molecules on the copper and silicon substrates with 0.6 keV Xe and SF_5 projectiles are performed. The yield-to-damage ratio, defined as the ratio of the number of molecules ejected stable and intact to the number of molecules ejected either fragmented or unstable, and the yield-to-disappearance ratio, defined as the ratio of the number of molecules ejected stable and intact to the total number of ejected molecules, are calculated by averaging the results of 150 trajectories for each projectile/substrate system. The greatest enhancements in the yield-to-damage ratio and the yield-to-disappearance ratio are on the open lattice substrate with the lighter mass atoms, ^{12}Si-(100). Polyatomic projectiles are able to increase the yield more than the damage because different types of motion are responsible for producing the two types of molecules. The average energy density distribution for each projectile/substrate system is calculated as a function of radial distance from the impact point. SF_5 is able to deposit its energy over the widest surface area on the silicon substrate, which leads to the greatest ejection of intact and stable molecules.

2. Method

The classical method of molecular dynamics simulations is used to study the systems of interest and the details are described extensively elsewhere.[48−50] Briefly, the initial conditions of the system and the potential energy functions to describe the interactions among the atoms are specified, and Hamilton's equations of motion are integrated to determine the position and velocity of each atom as a function of time. From the final positions and velocities of the atoms, the identity, kinetic energy, and internal energy of each ejected species are calculated. In addition, animations of the motions of the atoms during the bombardment event are analyzed in order to determine mechanisms for ejection.

The model systems consist of a monolayer of twenty biphenyl ($C_{12}H_{10}$) molecules adsorbed on copper and silicon substrates and are shown in Figure 1. The Cu(001) microcrystallite consists of 2574 atoms with 9 layers of 286 atoms. The Si(100)-(2×1) microcrystallite consists of 2520 atoms, with 9 layers of 280 atoms, and the top layer of silicon atoms is reconstructed into dimers. The positions of the biphenyl molecules are determined by allowing the adsorbates to equilibrate at 0 K on the substrate, using an algorithm based on the generalized Langevin equation (GLE).

The forces between the atoms are described by the best available potential energy functions.[51,52] The MD/CEM potential developed by DePristo et al.[53−55] is used for the Cu−Cu interactions, the Tersoff potential is used for the Si−Si interactions,[56] and Brenner's hydrocarbon potential is used for the C−C, C−H, and H−H interactions.[57,58] For the silicon[59] and hydrocarbon[40] potentials, Molière potentials are used in the repulsive region. The pairwise Cu−C, Cu−H, Si−C, and Si−H interactions between the atoms in the biphenyl molecules and the metal substrate are described by Lennard-Jones potentials[60]

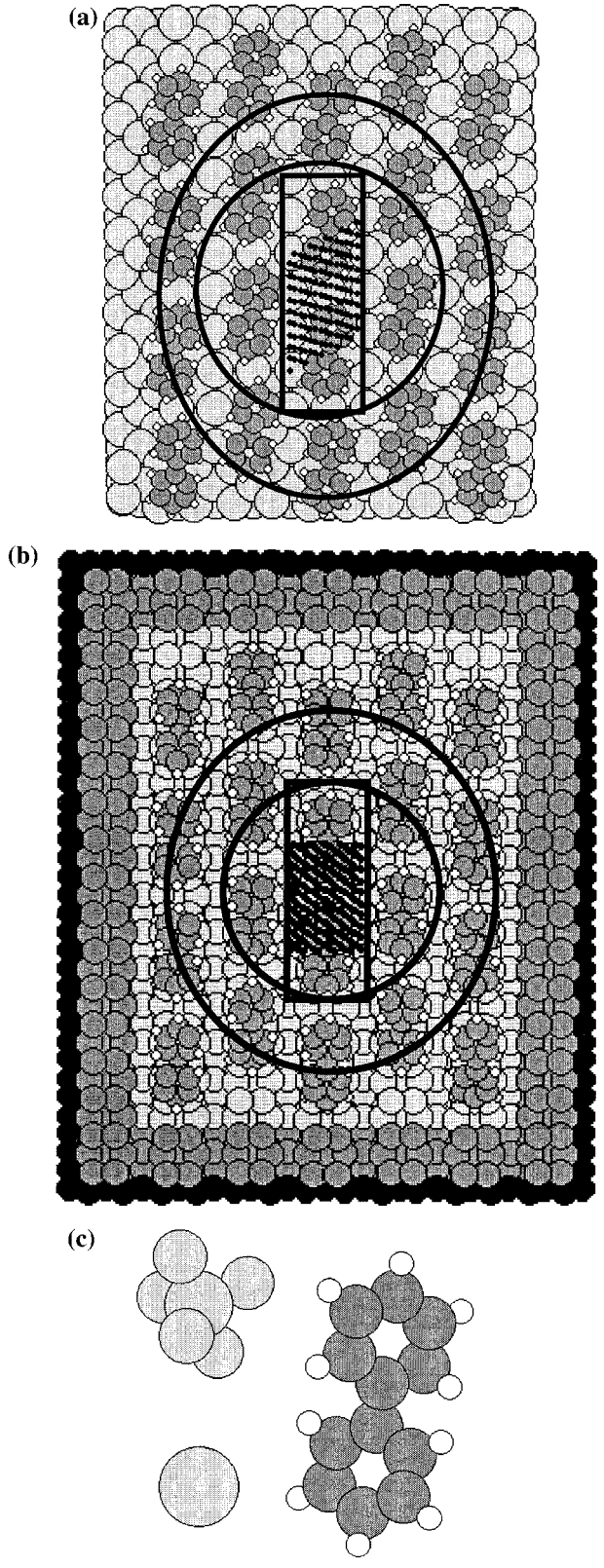

Figure 1. Top views of the model systems used in the simulations. (a) monolayer of biphenyl molecules on the Cu(001) microcrystallite, and (b) monolayer of biphenyl molecules on the Si(100)-(2 × 1) microcrystallite. The rectangular box outlines the two target molecules that overlap the impact zone of the bombarding projectile. The two circles outline the first and second rings of molecules surrounding the impact zone. The rhomboid-shaped collection of dots represents the 150 impact points of the projectile. The copper microcrystallite has dimensions of 37.2 Å × 45.0 Å and the silicon microcrystallite has dimensions of 53.8 Å × 65.3 Å. (c) Picture illustrating the sizes of the SF_5 and Xe projectiles relative to a biphenyl molecule.

with the form of the equation given in ref 40, using the following potential parameters: $\epsilon_{Cu-C} = 0.05$ eV, $\epsilon_{Cu-H} = 0.01$ eV, $\epsilon_{Si-C} = 0.05$ eV, and $\epsilon_{Si-H} =$,0.01 eV and $\sigma = 2.3$ Å for all the interactions. With these parameters, the binding energies of the biphenyl molecule to the copper and silicon substrates are 2.3 and 2.0 eV, respectively. Larger values than those in the experimental systems of interest are used in order to reduce the yield and conserve computer time. The absolute yield is not critical because the quantity of interest is the enhancement in yield with SF_5 compared to Xe. Simulations were performed in which the binding energy was changed to half the original value, and the same trends in the results were shown with the lower binding energy. A Molière potential[61] is used in the repulsive region of the potential for these interactions and is connected to the Lennard-Jones potential with a cubic spline function.

The Cu and SF_5 projectiles are brought in at normal incidence with 0.6 keV of energy. The orientation of the SF_5 projectile with respect to the surface is selected randomly. The results are calculated with each projectile for 150 trajectories, where each trajectory has a different aiming point on the surface, shown by the black points in Figure 1. The trajectory is terminated when the atoms left on the surface do not have enough energy to eject and the typical time ranges from to 0.2 to 5 ps. In the simulations, it was found that the edge layers of silicon atoms reconstructed into dimers as the integration of the trajectory proceeded, thereby releasing extra energy into the crystal. To prevent the reconstruction, the outer edge layer of atoms are held rigidly in place and three layers of stochastic atoms absorb energy from the microcrystallite. Artifacts due to particles or energy reflecting from the edges were carefully monitored to make sure that they did not affect the ejection yield.

The yield and damage are determined from the positions and velocities of the biphenyl molecules at the end of the trajectory. For each biphenyl molecule, there are five possible outcomes: (1) ejection as an intact stable molecule, (2) ejection as an intact unstable biphenyl molecule with enough energy to fragment before reaching the detector, (3) broken into fragments before the trajectory is terminated, (4) left intact but unstable on the surface, and (5) left undisturbed on the surface. The yield of biphenyl molecules out of 150 trajectories is calculated as the total number of stable biphenyl molecules ejected from the surface. Biphenyl molecules are defined to be stable when the internal energy is less than 10 eV and unstable when the internal energy is greater than 10 eV. In experiments, these unstable molecules would not survive intact within 10 μs, the typical time it would take to reach a detector. As discussed elsewhere, RRK calculations estimate that this is a reasonable value.[46] Furthermore, simulations were performed with biphenyl molecules that had internal energies ranging from 0 to 15 eV and molecules with 10 eV internal energy or less did not fragment after 2 ns.

The damage reflects the number of molecules that are not detected as yield, but are damaged so that they are no longer available for future analysis. To estimate the number of unstable intact molecules left on the surface, the energy of each intact molecule remaining on the surface is calculated and molecules with internal energies greater than 10 eV are counted as unstable. The number of intact unstable molecules left on the surface was found negligible, and therefore, the damage is defined simply as the sum of the number of ejected unstable and fragmented molecules. The yield-to-damage ratio is calculated as the ratio of the yield to the damage. Another quantity, the yield-to-disappearance ratio, is more comparable to the experimental

TABLE 1: Average Number of Stable (S), Unstable (U), and Fragmented (F) Molecules out of 150 Trajectories[a]

system	*S*	*E*[*Y*]	*U*	*F*	*Y*/*D*	*E*[*Y*/*D*]	*Y*/(*Y* + *D*)	*E*[*Y*/(*Y* + *D*)]
SF_5/Cu(001)	1.7	1.2	0.5	1.4	0.9	0.6	0.46	0.8
Xe/Cu(001)	1.3		0.1	0.8	1.5		0.60	
SF_5/Si(100)	2.6	2.5	0.2	1.4	1.6	1.2	0.62	1.1
Xe/Si(100)	1.0		0.04	0.7	1.3		0.57	
SF_5/^{12}Cu(001)	1.5	2.9	0.8	1.0	0.9	1.7	0.47	1.4
Xe/^{12}Cu(001)	0.5		0.3	0.7	0.5		0.34	
SF_5/^{12}Si(100)	1.9	3.9	0.5	0.9	1.3	2.5	0.57	1.6
Xe/^{12}Si(100)	0.5		0.2	0.7	0.5		0.35	
SF_5/^{64}Si(100)	1.8	1.7	0.9	1.6	0.7	0.7	0.41	0.8
Xe/^{64}Si(100)	1.0		0.3	0.8	1.0		0.50	

[a] The yield-to-damage ratio (*Y*/*D*) and yield-to-disappearance (*Y*/(*Y* + *D*)) ratio are calculated. Enhancement factors, defined as the ratio with SF_5 to that with Xe, are shown for the stable molecules (*E*[*Y*]), the yield-to-damage ratio (*E*[*Y*/*D*]) and the yield-to-disappearance ratio (*E*[*Y*/(*Y* + *D*)]).

definition of damage cross section. It is calculated as the ratio of yield to the sum of the yield and damage.

3. Results and Discussion

The enhancements in the yield, the yield-to-damage ratio, and the yield-to-disappearance ratio depend on the lattice type and mass of the substrate, and these results are explained in terms of the mechanisms for ejection and the energy density distribution. First, the enhancements in the yield, the yield-to-damage ratio, and the yield-to-disappearance ratio are analyzed as a function of the structure and mass of the substrate. Then, the mechanisms for the production of fragmented, unstable, and stable molecules are described. The distribution of energy density deposited by the projectile onto the substrate is analyzed for each system and is used to explain why the enhancement in yield with SF_5 differs on the silicon and copper substrates. Finally, the dependence of the kinetic energy distribution of the ejected molecules on the substrate is discussed.

3.1. Effect of Lattice Structure and Mass on the Enhancements in Yield, Yield-to-Damage Ratio, and Yield-to-Disappearance Ratio. The average number of stable (S), unstable (U), and fragmented (F) biphenyl molecules reported for the SF_5 and Xe projectiles on the Cu(001) and Si(100) substrates are given in Table 1. The average number is calculated as the raw number of molecules divided by 150, the total number of trajectories. A greater number of biphenyl molecules ejected intact and stable is obtained with SF_5 bombardment compared to Xe bombardment. Moreover, the enhancement of yield *E*[*Y*], is greater for the silicon substrate than the copper substrate. The issue for analysis, however, is whether the useful signal is enhanced with polyatomic cluster bombardment. Thus, the damage created by both SF_5 and Xe bombardment is important. As shown in Table 1, more damage is created by SF_5 than Xe on both substrates. By calculating the ratio of (*Y*/(*Y* + *D*)), where *D* represents the damage due to unstable molecule ejection and fragment molecules, the enhancement of useful signal can be estimated. For the Si substrate, the SF_5 bombardment does increase the yield more than the damage compared to Xe bombardment. For the Cu substrate, on the other hand, Xe enhances the yield-to-damage ratio more than SF_5.

The two substrates differ in two ways: silicon atoms have a lighter mass than copper atoms and silicon is a network covalent solid with a more open lattice than the densely packed face-centered cubic structure of copper. By comparing substrates with the same mass but different structures, the effect of the lattice structure can be isolated. Therefore, simulations were performed on substrates in which only the mass, but not the identity, of the atoms was changed. The mass of silicon was changed to 64 amu in the ^{64}Si(100) substrate to have the same mass as copper. The mass of silicon and copper atoms was changed to 12 amu in the ^{12}Si(100) and ^{12}Cu(001) substrates to have the same mass as carbon. The enhancement in yield with SF_5 is greater on ^{64}Si(100) than on Cu(001) and greater on ^{12}Si(100) than on ^{12}Cu(001), which indicates that the lattice structure is important for yield enhancement. The enhancement factors for the yield-to-damage and the yield-to-disappearance ratios are greater on the ^{12}Si(100) substrate than on the ^{12}Cu(001) substrate, but are about the same on the ^{64}Si(100) and Cu(001) substrates.

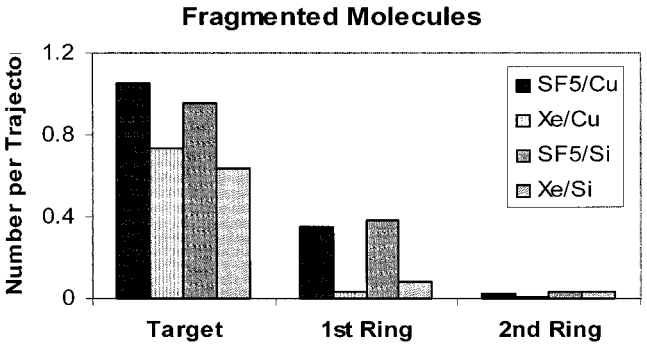

Figure 2. Average number of ejected fragmented molecules from the Si(100) and Cu(001) substrates as a function of distance from target zone. Figure 1 shows how the molecules on the surface are categorized by their location.

Evidently, the mass of the substrate atoms must also be an important factor. The yield, yield-to-damage ratio, and the yield-to-disappearance ratio are greatest on the Si(100) substrate, which has a mass closest to the mass of the atoms in the SF_5 projectile. When there is mass matching between the projectile atoms and the substrate atoms, the projectile can transfer the greatest amount of energy to the substrate atoms. When the projectile atom (or atoms) are much heavier than the substrate atoms, the projectile penetrates directly through the lattice and is not able to transfer energy to the top layers of atoms. Preliminary experiments by Gillen et al. supports this concept of mass matching.[62] They performed depth profiles of glutamate, an amino acid, with C_8^- and Al_7^- clusters and found the carbon clusters to be more effective. Although the yield, the yield-to-damage ratio, and the yield-to-disappearance ratio are greatest on the Si(100) substrate, the greatest enhancements are on the ^{12}Si(100) substrate. This is because the numerator in the enhancement ratio is so small. Many of the trajectories with Xe on ^{12}Si(100) result in no ejected molecules because of the open lattice structure and light mass of the atoms. The Xe projectile often penetrates the lattice to the bottom of the microcrystallite without transferring much of its energy to the substrate atoms.

3.2. Mechanisms for Production of Damaged and Yield Molecules. Molecules that are fragmented during the course of the trajectory make up the major contribution to the total number of damaged molecules. As shown in Figure 1, the location of the molecules can be divided into three categories: (1) the two molecules in the target zone outlined by the black rectangle, (2) the four molecules in the first outer ring from the target zone, and (3) the eight molecules in the second outer ring from the target zone. For the copper substrate, the average distance to the closest impact point is 5 Å for molecules in the first ring and 10 Å for molecules in the second ring. For the silicon substrate, the distances are 5 Å for the first ring and 11 Å for the second ring. In Figure 2, the average number of fragmented molecules for each projectile/substrate system is shown as a

function of distance from the target zone. The primary mechanism for fragmentation is the bombarding projectile directly striking a molecule as it impacts the surface, which is also the case in molecular dynamics simulations by Delcorte et al. of the bombardment of a monolayer of polystyrene molecules on silver with 0.5 keV Ar atoms.[47] A secondary mechanism for fragmentation also occurs in which fragments from the directly struck target molecules move laterally and strike neighboring molecules, causing them to fragment. Molecules are not observed to fragment by collision cascades of the substrate atoms. The fact that molecules outside the target zone are fragmented is in agreement with earlier simulations performed by Winograd, Garrison, and Harrison. They studied the bombardment of a monolayer of CO on a Ni(001) microcrystallite with 0.6 keV Ar atoms and found that only 10−15% of the molecules ejected dissociatively, and some of these are outside of the target zone.[63]

Most of the fragmented molecules are in the target zone. With SF_5, on average one of the two target molecules is fragmented by each impact. With Xe, this number is slightly smaller because of the smaller size of the projectile. A much smaller contribution to the number of fragmented molecules is from molecules in the first ring, and a negligible contribution is from molecules in the second ring. SF_5 has many more fragmented molecules from the first outer ring than Xe. There are two reasons for this. First, since SF_5 is larger, it affects a wider area of molecules as it impacts the surface. Furthermore, when SF_5 breaks up, it causes lateral motion of the biphenyl fragments, which then hit molecules farther away.

An interesting result of this mechanism is the formation of products that are composed of atoms from two or more different molecules. A molecule or molecular fragment that is initially struck by the incoming particle moves in a lateral direction and combines with a neighboring molecule or molecular fragment to make a new species. Examples of such products are H and H to form H_2, $C_{12}H_9$ and H to form $C_{12}H_{10}$, and $C_{12}H_9$ and CH to form $C_{13}H_{10}$. Some of these products formed by rearrangements are misleading because they do not reflect the structure of the original molecules to be analyzed. In agreement with experimental observations by Van Stipdonk and co-workers,[15−21] SF_5 produces substantially more of these rearranged products than Xe: SF_5/Cu has 58, Xe/Cu has 9, SF_5/Si has 70, and Xe/Si has 15.

A minor contribution to the damaged molecules is unstable molecules that are ejected intact, but have enough internal energy to fragment before reaching the detector. SF_5 produces a greater number of unstable molecules than Xe, and SF_5 on Cu(001) produces twice as many unstable molecules as SF_5 on Si(100). In Figure 3, the yield of unstable molecules is plotted as a function of the center of mass of the molecule from the impact point. To generate this plot, the distance between the impact point and each unstable biphenyl molecule was histogrammed in 2 Å increments. Therefore, the value at 7 Å is the average number of unstable molecules that were originally a distance between 6 and 8 Å from the impact point of the trajectory. The unstable molecules are farther from the impact point than fragmented molecules, but are generally closer to the target than stable ejected molecules. As in the case with fragmented molecules, the predominant mechanism for the ejection of unstable molecules is by the downward impact of the projectile. However, with unstable molecules, the primary particle will nudge the molecule as it comes down rather than directly strike it in its center. This occurs more often with SF_5 than with Xe because it is larger. Energetic upward moving

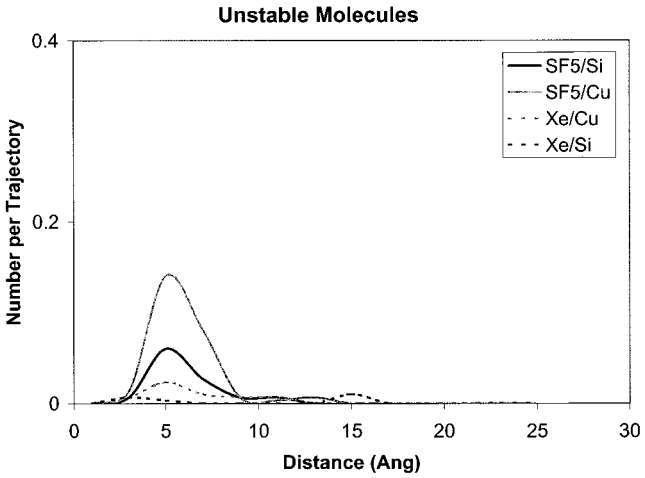

Figure 3. Average number of ejected unstable molecules on the Si(100) and Cu(001) substrates as a function of distance from the impact point. Unstable molecules are ejected with greater than 10 eV of internal energy and are predicted to fragment within 10 μs before reaching an experimental detector.

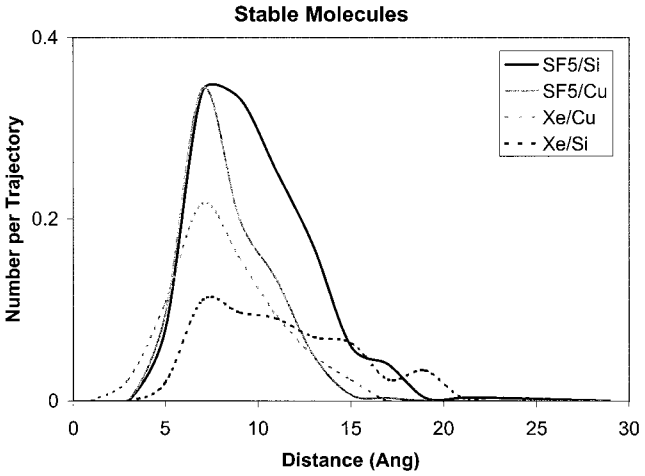

Figure 4. Average number of ejected stable molecules as a function of distance from the impact point.

substrate atoms also play a role in ejecting unstable molecules. SF_5 gives more energy to the atoms in the top two layers of the substrate than Xe, and therefore, produces more unstable molecules. Additionally, there is a mechanism unique to the SF_5 projectile. When SF_5 breaks apart in the substrate, the individual S and F atoms recoil and can hit molecules from underneath, causing molecules to eject with enough energy to be unstable. SF_5 tends to break up much closer to the top of the surface on the copper substrate, and therefore, produces more unstable molecules than on the silicon substrate.

Stable whole molecules are ejected by the action of upward moving substrate atoms that hit the molecules from below and gently lift them off of the surface. In Figure 4, the average number of stable molecules per trajectory is plotted as a function of distance of the center of mass of the molecule from the impact point of the primary particle. The intensity of the yield curves is greater with SF_5 than with Xe, and the curves are broader on silicon than on copper. SF_5 produces about the same number of ejected molecules on copper and silicon near the impact point. However, the overall yield with SF_5 on silicon is much greater because of the breadth of the curve.

The curves are broader on silicon than copper because silicon has a more open lattice structure. On the copper substrate, SF_5 breaks up on impact and the S and F atoms recoil from the

surface without penetrating below the first layer of substrate atoms. On the silicon substrate, SF_5 is able to penetrate to the second or third layer of substrate atoms before breaking apart because of the open nature of lattice. When SF_5 breaks up within the lattice rather than on it, the projectile produces a greater number of upward moving substrate atoms, which lead to a greater yield of biphenyl molecules.[37]

An important question is how is it possible for SF_5 to enhance the number of yield molecules without producing a corresponding increase in the number of damaged molecules. The underlying reason for this is that different types of motion are responsible for the production of damaged and yield molecules. Molecules are primarily damaged by the downward and sideways motion of the primary projectile and ejected biphenyl molecules and fragments, while yield molecules are ejected by the upward motion of the substrate atoms. With the open lattice structure and the lighter mass atoms, SF_5 is able to produce upward moving substrate atoms over a more delocalized area. By localizing the damage to only molecules near the impact point and delocalizing the area of ejected molecules, SF_5 is able to enhance the yield more than the damage.

3.**3. Energy Density Distribution on the Surface.** The energy density distribution with the two projectiles on the two different substrates has been analyzed to understand its relationship to the yield. The motion of the upward moving substrate atoms is responsible for the ejection of yield molecules, and therefore, only the contribution from these atoms is included in the energy density calculations. To calculate the energy density distribution, the surface area is divided up into 2 Å × 2 Å bins. The total kinetic energy of all moving upward substrate atoms in the bin that are within 2 Å above the surface is determined at each time step of the trajectory. Substrate atoms are considered to be moving upward if the velocity component in the upward direction is positive. The maximum kinetic energy in each bin over time for each trajectory is then recorded. The energy density is in units of eV per the volume of the bin, which is 8 $Å^3$. To save computer time, the energy density is averaged over only 75 of the 150 trajectories. These are the 75 trajectories with impact points in the left half of the impact zone.

The radial distribution of the average energy density is plotted in Figure 5a. To calculate the radial distribution, the energy density is summed over the bins around each ring at a fixed distance from the impact point. The magnitude of the energy density is greater on the copper substrate than on the silicon substrate. If the intensity was the only factor, then the yields should be greatest on copper. However, the yield with SF_5 is greater on silicon than on copper, and therefore, the intensity alone cannot explain the difference in yields. With silicon, the peaks are shifted toward longer distances from the impact point and the curves are broader because silicon is less dense than copper. The greater breadth of energy density on silicon corresponds to the greater breadth of the yield curves in Figure 4. Therefore, it is the greater area over which the energy density is distributed that leads to the greater yield on the silicon substrate.

Figure 5a illustrates that an increase in the energy density does not necessarily result in an increase in the molecular yield. If a minimum threshold of energy is required to eject a molecule, then any energy in excess of this amount is unnecessary and may actually be counterproductive by causing damage to the biphenyl molecules. Calculations were performed in order to estimate the magnitude of the energy threshold. The total kinetic energy of the upward moving substrate atoms in a volume underneath each biphenyl molecule was calculated as the

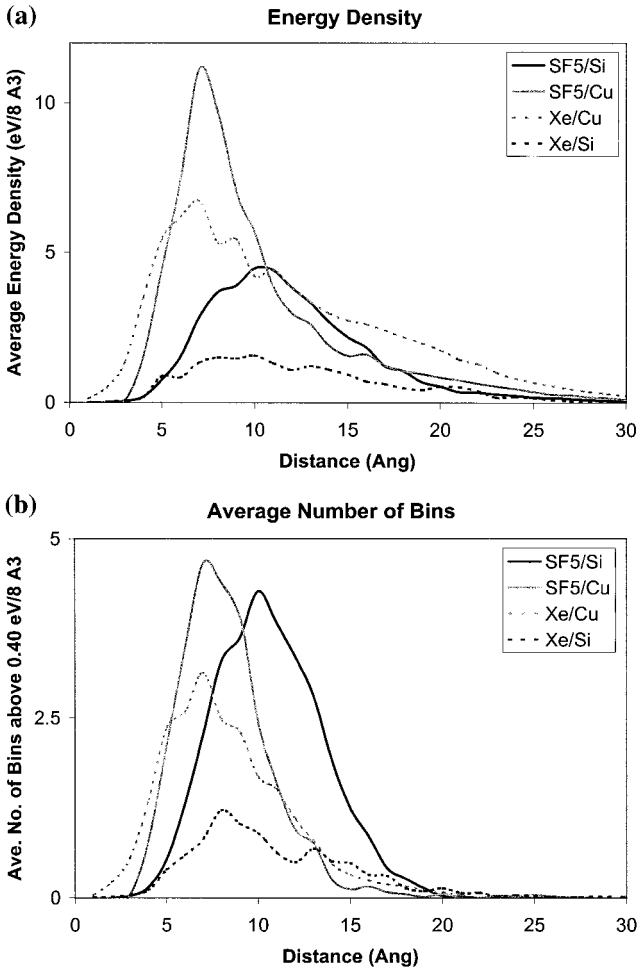

Figure 5. (a) Average energy density as a function of distance from the impact point. Only kinetic energy from upward moving substrate atoms is included in the calculation, and details are described in the text. (b) Average number of bins with energy above 0.40 eV as a function of distance from the impact point. The value of 0.40 eV is approximately the minimum threshold energy of the substrate atoms needed to eject a molecule. Therefore, the number of bins with energy greater than this value correlates with the surface area of the substrate that is effective for desorption.

trajectory evolved in time and the maximum energy was recorded. If an absolute value of the energy threshold existed, then the maximum kinetic energy of the substrate atoms in the volume beneath every ejected biphenyl molecule would be above a definite value. However, the simulations demonstrate that this is not the case; the energy needed depends on the atomistic motions leading to ejection of the molecule and varies with each trajectory. It was found that the maximum kinetic energy of the substrate atoms in the volume underneath 90% of the ejected molecules was greater than 0.50 eV on the copper substrate and greater than 0.40 eV on the silicon substrate. Therefore, the minimum energy of the substrate atoms needed to eject the biphenyl molecule is estimated to be 0.40 eV.

Using this value for the threshold, it can be hypothesized that any bin with energy density greater than 0.40 eV/8 $Å^3$ will be effective in ejecting a molecule. This is a reasonable assumption because a bin has about the same surface area as the ring of a biphenyl molecule. The number of bins with energy density greater than this threshold correlates with the surface area of the substrate that is effective for desorption. In Figure 5b, the average number of bins with energy density greater than 0.40 eV/8 $Å^3$ is plotted as a function of distance from the impact

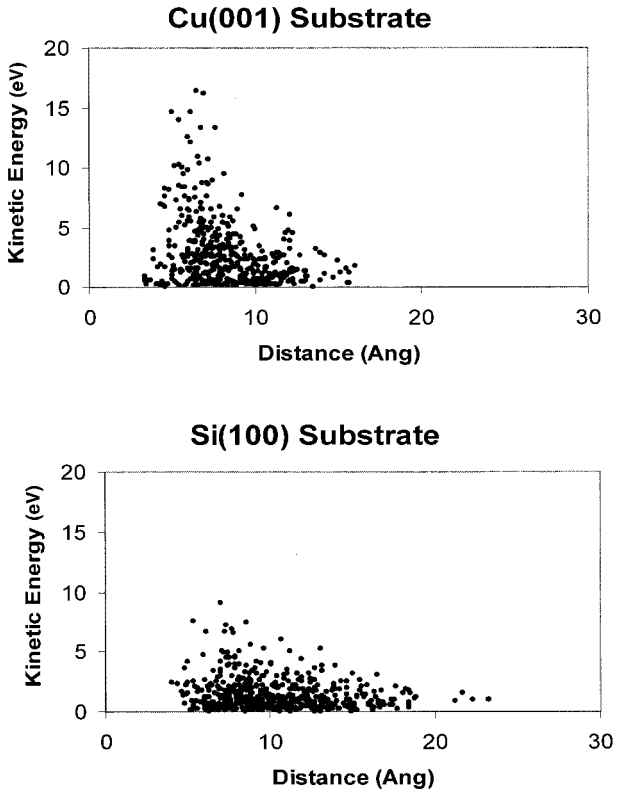

Figure 6. Center of mass kinetic energy distribution of ejected stable molecules as a function of distance from the impact point. (a) Total with Xe and SF_5 projectiles on Cu(001) substrate, and (b) total with Xe and SF_5 projectiles on Si(100) substrate.

point for each projectile/substrate system. SF_5 on the silicon substrate has the greatest number of bins, the greatest effective area, and thus, the greatest yield. Furthermore, there are a greater number of bins with SF_5 on silicon farther away from the impact point, where there are a greater number of biphenyl molecules. The key to the enhancement in yield with SF_5 on the silicon substrate is that the energy density is deposited over a wider area of the surface.

3.4. Kinetic Energy Distribution of Yield Molecules. Energy density in excess of the minimum threshold is not effective in producing more ejected molecules. Rather, the extra energy is deposited into the kinetic and internal energy of the ejected molecules. Since the energy density is greater on copper, molecules ejected from the copper substrate have more kinetic energy than those ejected from the silicon substrate. In Figure 6, the center of mass kinetic energy of each stable biphenyl molecule is plotted as a function of distance from the impact point. The distribution of the biphenyl molecules ejected with the Xe and SF_5 projectiles from the copper substrate is shown in Figure 6a, and the distribution from the silicon substrate is in Figure 6b. As the distance from the impact point increases, the kinetic energy of the molecule decreases because there is less energy transferred to the molecule from the substrate atoms. Molecules close to the impact have much higher kinetic energy from the copper substrate than from the silicon substrate. The higher mass of the copper atoms imparts more momentum to the ejected biphenyl molecules, but does not cause a larger number to be ejected.

4. Conclusions

Molecular dynamics simulations have been performed on a monolayer of biphenyl molecules with SF_5 and Xe projectiles on two different substrates, Si(100) and Cu(001), with the purpose of understanding how polyatomic projectiles can improve the sensitivity of organic SIMS. The enhancements in the yield, in the yield-to-damage ratio, and in the yield-to-disappearance ratio have been determined for each projectile/substrate system. The correlation between the yield and the energy density distribution on the surface has been analyzed.

The yield of ejected stable molecules is greater with SF_5 than with Xe on both substrates. The degree of enhancement in yield depends on the structure of the substrate and on the mass of the substrate atoms. Molecules are ejected whole and stable by the upward motion of substrate atoms, which lift the molecules gently off the surface. SF_5 is most effective on silicon, which is a network covalent solid and has a more open lattice structure. The more open lattice structure allows SF_5 to break up within the substrate rather than on the top surface of the substrate, which is illustrated in Figure 1 of ref 37. The breakup of SF_5 within the lattice initiates collision cascades that have an upward momentum underneath the biphenyl molecules, which can lift them intact off the surface. When the mass of the projectile atom (or atoms) is close to the mass of the substrate atoms, the greatest amount of energy is transferred to the top layers of atoms, which leads to a greater yield of ejected molecules. The results of the simulations are consistent with the recent results of Stapel et al.,[64] who have studied the bombardment of a monolayer organic film on a silver substrate with 0.50 keV Xe and SF_5 projectiles. At these lower energies, the yield and efficiency with Xe was higher than with SF_5. Silver atoms are much heavier than copper atoms, and therefore, the close-packed structure and mass matching should cause a higher yield with Xe than with SF_5.

The number of damaged molecules is greater with SF_5 than with Xe on both substrates. There are two types of damaged molecules: molecules that are directly fragmented during the progress of the trajectory and a smaller number of unstable molecules that are ejected intact with enough energy to fragment within 10 μs, before reaching an experimental detector. The most common mechanism for unstable and fragmented molecules is the primary particle striking the molecule as it impacts the surface.

Since the mechanisms responsible for producing yield and damaged molecules are different, it is possible for the polyatomic projectile to increase the molecular yield more than the number of damaged molecules. SF_5 on the silicon substrate is able to delocalize the area of ejected molecules while keeping a fairly localized area of damaged molecules. Therefore, the enhancement factors for the yield-to-damage ratio and the yield-to-disappearance ratio are greater than 1 on the silicon substrate. The greatest enhancement in yield, the yield-to-damage ratio, and the yield-to-disappearance ratio is on ^{12}Si(100), the open lattice structure with the lightest mass. Therefore, our simulations predict that polyatomic projectiles will show the greatest enhancements on bulk molecular solids composed of lighter mass atoms and an open lattice structure. For example, graphite or diamond would be the optimal matrix for static SIMS of organic monolayers using a SF_5^+ primary ion beam.

The energy density distribution of the upward moving substrate atoms has been analyzed. There is a greater amount of energy density on the copper substrate than on the silicon substrate. However, what is important in determining the yield is the relative intensity and area of energy density on the surface. SF_5 on the silicon substrate distributes energy density above a certain minimum threshold over the widest area, and therefore, produces the greatest yield of ejected stable molecules.

Acknowledgment. The financial support of the National Science Foundation, the Petroleum Research Fund and the Research Corporation is gratefully acknowledged. Computing facilities were provided by grants from the National Science Foundation and the IBM Selected University Research Program at the Center for Academic Computing of The Pennsylvania State University. In addition, we thank Arnaud Delcorte, Michael Van Stipdonk, Nick Winograd, Anthony Appelhans, and Greg Gillen for insightful discussions about this work and Jeff Nucciarone for assistance with the computations.

References and Notes

(1) Benninghoven, A.; Rudenauer, F. G.; Werner, H. W. *Secondary Ion Mass Spectrometry*; Wiley: New York, 1987; Chapter 2.2.5.

(2) *Secondary Ion Mass Spectrometry—Principles and Applications*; Vickerman, J. C., Brown, A., Reed, N. M., Eds.; Oxford University Press: New York, 1989; pp 1−71, 149−243.

(3) Winograd, N.; Garrison, B. J In *Ion Spectroscopies for Surface Analysis*; Czanderna, A. W., Hercules, D. M., Eds.; Plenum Press: New York, 1991; pp 45−141.

(4) Winograd, N. *Anal. Chem*. **1993**, *65*, 622A.

(5) Benninghoven, A.; Hagenhoff, B.; Niehuis, E. *Anal. Chem*. **1993**, *65*, 630A.

(6) Appelhans, A. D.; Delmore, J. E. *Anal. Chem.* **1989,** *61*, 1087.

(7) Groenewald, G. S.; Delmore, J. E.; Olson, J. E.; Appelhans, A. D.; Ingram, J. C.; Dahl, D. A. *Int. J. Mass Spectrom. Ion Processes* **1997**, *163*, 185.

(8) Groenewold, G. S.; Gianotto, A. K.; Olson, J. E.; Appelhans, A. D.; Ingram, J. C.; Delmore, J. E.; Shaw, A. D. *Int. J. Mass Spectrom. Ion Processes* **1998,** *174*, 129.

(9) Blain, M. G.; Della-Negra, S.; Joret, H.; Le Beyec, Y.; Schweikert, E. A. *Phys. Rev. Lett*. **1989**, *63*, 1625.

(10) Schweikert, E. A.; Blain, M. G.; Park, M. A.; Da Silveira, E. F. *Nucl. Instrum. Methods Phys. Res., Sect. B* **1990**, *50*, 307.

(11) Benguerba, M.; Brunelle, A.; Della-Negra, S.; Depauw, J.; Joret, H.; Le Beyec, Y.; Blain, M. G.; Schweikert, E. A.; Ben Assayag, G.; Sudraud, P. *Nucl. Instrum. Methods Phys. Res., Sect. B* **1991**, *62*, 8.

(12) Barros Leite, C. V.; da Silveira, E. F.; Jeronymo, J. M. F.; Pinho, R. R.; Baptista, G. B.; Schweikert, E. A.; Park, M. A. *Phys. Rev. B* **1992**, *45*, 12218.

(13) Boussofiane-Baudin, K.; Bolbach, G.; Brunelle, A.; Della-Negra, S.; Håkansson, P.; Le Beyec, Y. *Nucl. Instrum. Methods Phys. Res., Sect. B* **1994**, *88*, 160.

(14) Demirev, P. A.; Eriksson, J.; Zubarev, R. A.; Papaléo, R.; Brinkmalm, G.; Håkansson, P.; Sundqvist, B. U. R. *Nucl. Instrum. Methods Phys. Res., Sect. B* **1994**, *88*, 138.

(15) Van Stipdonk, M. J.; Harris, R. D.; Schweikert, E. A. *Rapid Commun. Mass Spectrom*. **1997**, *11*, 1794.

(16) Van Stipdonk, M. J.; Justes, D. R.; Santiago, V.; Schweikert, E. A. *Rapid Commun. Mass Spectrom*. **1998**, *12*, 1639.

(17) Harris, R. D.; Van Stipdonk, M. J.; Schweikert, E. A. *Int. J. Mass Spectrom. Ion Processes* **1998**, *174*, 167.

(18) Van Stipdonk, M. J.; Santiago, V.; Schweikert, E. A. *J. Mass Spectrom.* **1999**, *34*, 554.

(19) Diehnelt, C. W.; Van Stipdonk, M. J.; Schweikert, E. A. *Phys. Rev. A* **1999**, *59*, 4470.

(20) Harris, R. D.; Baker, W. S.; Van Stipdonk, M. J.; Crooks, R. M.; Schweikert, E. A. *Rapid Commun. Mass Spectrom.* **1999**, *13*, 1374.

(21) Van Stipdonk, M. J.; English, R. D.; Schweikert, E. A. *J. Phys. Chem. B* **1999**, *103*, 7929.

(22) Hand, O. W.; Majumdar, T. K.; Cooks, R. G. *Int. J. Mass Spectrom. Ion Processes* **1990**, *97*, 34.

(23) Mahoney, J. F.; Perel, J.; Ruatta, S. A.; Martino, P. A.; Husain**,** S.; Lee, T. D. *Rapid Commun. Mass Spectrom.* **1991,** *5*, 441.

(24) Mahoney, J. F.; Parilis, E. S.; Lee, T. D. *Nucl. Instrum. Methods Phys. Res., Sect. B* **1994**, *88*, 154.

(25) Le Beyec, Y. *Int. J. Mass Spectrom. Ion Processes* **1998**, *174*, 101.

(26) Kötter, F.; Benninghoven, A. *Appl. Surf. Sci.* **1998**, *133*, 47.

(27) Stapel, D.; Brox, O.; Benninghoven, A. *Appl. Surf. Sci.* **1999**, *140*, 156.

(28) Ada, E. T.; Hanley, L. *Int. J. Mass Spectrom. Ion Processes* **1998**, *174*, 231.

(29) Gillen, G.; Roberson, S. *Rapid Commun. Mass Spectrom.* **1998**, *12*, 1303.

(30) Gillen, G.; King, R. L.; Chmara, F. *J. Vac. Sci. Technol., A* **1999**, *17*, 845.

(31) Gillen, G.; Walker, M.; Thompson, P.; Bennett, *J. Vac. Sci. Technol., B* **2000**, *18*, 503.

(32) Todd, Peter J.; Mcmahon, J. M.; Mccandlish, C. A., Jr. In Proceedings of the 45th ASMS Conference on Mass Spectrometry and Allied Topics, Palm Springs, CA, June 1−5, 1997.

(33) Benninghoven, A. In I*on Formation from Organic Solids, Springer-Verlag Series in Chemical Physics 25*; Benninghoven, A., Ed.; Springer-Verlag: Berlin, 1983; p 77.

(34) Zaric, R.; Pearson, B.; Krantzman, K. D.; Garrison, B. J. *Int. J. Mass Spectrom. Ion Processes* **1998**, *174*, 155.

(35) Zaric, R.; Pearson, B.; Krantzman, K. D.; Garrison, B. J. In *Secondary Ion Mass Spectrometry, SIMS XI*; Lareau, R., Gillen, G., Eds.; John Wiley and Sons: New York, 1998; pp 601−604.

(36) Townes, J. A.; White, A. K.; Krantzman, K. D.; Garrison, B. J. *Proceedings for the 15th International Conference on the Application of Accelerators in Industry*; Duggan, J. L., Morgan, I. L., Eds.; American Institute of Physics: New York, 1999; pp 401−404.

(37) Townes, J. A.; White, A. K.; Wiggins, E. N.; Krantzman, K. D.; Garrison, B. J.; Winograd, N. *J. Phys. Chem. B* **1999**, *103*, 4587.

(38) Ward, D.; Nguyen, T. C.; Krantzman, K. D.; Garrison, B. J. *Secondary Ion Mass Spectrometry, SIMS XII Proceedings*, **2000**, in press.

(39) Taylor, R. S.; Garrison, B. J. *J. Am. Chem. Soc.* **1994**, *116*, 4465.

(40) Taylor, R. S.; Garrison, B. J. *Langmuir* **1995**, *11*, 1220.

(41) Taylor, R. S.; Garrison, B. J. *Chem. Phys. Lett.* **1994**, *230*, 495.

(42) Taylor, R. S.; Garrison, B. J. *Int. J. Mass Spectrom. Ion Processes* **1995**, *143*, 225.

(43) Chatterjee, R.; Postawa, Z.; Winograd, N.; Garrison, B. J. *J. Phys. Chem. B* **1999**, *103*, 151.

(44) Liu, K. S. S.; Yong, C. W.; Garrison, B. J.; Vickerman, J. C. *J. Phys. Chem. B* **1999**, *103*, 3195.

(45) Garrison, B. J.; Delcorte, A.; Krantzman, K. D. *Acc. Chem. Res.* **2000**, *33*, 69.

(46) Delcorte, A.; Vanden Eynde, X.; Bertrand, P.; Vickerman, J. C.; Garrison, B. J. *J. Phys. Chem. B* **2000**, *104*, 2673.

(47) Delcorte, A.; Segda, B. G.; Garrison, B. J.; Bertrand, P. *Nucl. Instrum. Methods Phys. Res., Sect. B*, in press.

(48) Bernardo, D. N.; Bhatia, R.; Garrison, B. J. *Comput. Phys. Commun.* **1994**, *80*, 259.

(49) Garrison, B. J.; Winograd, N. *Science* **1982**, *216*, 805.

(50) Garrison, B. J. *Chem. Soc. Rev.* **1992**, *21*, 155.

(51) Garrison, B. J.; Kodali, P. B. S.; Srivastava, D. *Chem. Rev.* **1996**, *96*, 1327.

(52) Garrison, B. J.; Srivastava, D. *Annu. Rev. Phys. Chem.* **1995**, *46*, 373.

(53) Stave, M. S.; Sanders, D. E.; Raeker, T. J.; DePristo, A. E. *J. Chem. Phys.* **1990**, *93*, 4413.

(54) Raker, T. J.; DePristo, A. E. *Int. Rev. Phys. Chem.* **1991**, *10*, 1.

(55) Kelchner, C. L.; Halstead, D. M.; Perkins, L. S.; Wallace, N. M.; DePristo, A. E. *Surf. Sci.* **1994**, *310*, 425.

(56) Tersoff, J.; *Phys. Rev. B* **1988**, *37*, 6991.

(57) Brenner, D. W. *Phys. Rev. B* **1990**, *42*, 9458.

(58) Brenner, D. W.; Harrison, J. A.; White, C. T.; Colton, R. J. *Thin Solid Films* **1991**, *206*, 220.

(59) Smith, R.; Harrison, D. E., Jr.; Garrison, B. J. *Phys. Rev. B* **1989**, *40*, 93.

(60) Allen, M. P.; Tildesley, D. J. *Computer Simulations in Liquids*; Oxford University Press: Oxford, 1987; p 9.

(61) O'Connor, D. J.; MacDonald, R. J. *Radiat. Eff.* **1977**, *34*, 247−250.

(62) Gillen, G.; Freibaum, B.; Roberson, S. *Organic SIMS Using Polyatomic and Cluster Primary Ion Beams*; SIMS XII, Brussels, Belgium, September 7−12, 1999.

(63) Winograd, N.; Garrison, B. J.; Harrison, D. E., Jr. *J. Chem. Phys.* **1980**, *73*, 3473.

(64) Stapel, D.; Benninghoven, A. Proceedings of the 13th Annual SIMS Workshop, Lake Tahoe, California, April 30−May 3, 2000.